

**A STUDY OF COUPLED ROTOR-FUSELAGE VIBRATION
WITH HIGHER HARMONIC CONTROL USING
A SYMBOLIC COMPUTING FACILITY**

I. Papavassiliou^[i],
C. Venkatesan^[ii],
P. P. Friedmann^[iii].

Mechanical, Aerospace, and Nuclear Engineering Department
University of California, Los Angeles, CA 90024

Abstract

A fundamental study of vibration prediction and vibration reduction in helicopters using active controls was performed. The nonlinear equations of motion for a coupled rotor / flexible fuselage system have been derived using computer algebra on a special purpose symbolic computing facility. The details of the derivation using the MACSYMA program are described. The trim state and vibratory response of the helicopter are obtained in a single pass by applying the harmonic balance technique and simultaneously satisfying the trim and the vibratory response of the helicopter for all rotor and fuselage degrees of freedom. The influence of the fuselage flexibility on the vibratory response is studied. It is shown that the conventional single frequency higher harmonic control (HHC) capable of reducing either the hub loads or only the fuselage vibrations but not both simultaneously. It is demonstrated that for simultaneous reduction of hub shears and fuselage vibrations a new scheme called multiple higher harmonic control (MHHC) is required. The fundamental aspects of this scheme and its uniqueness are described in detail, providing new insight on vibration reduction in helicopters using HHC.

Nomenclature

a	Rotor blade lift curve slope
ACX, ACY, ACZ	Acceleration components at the fuselage C.G. with HHC in the x, y, z directions, respectively
ACXb, ACYb, ACZb	Baseline acceleration components at the fuselage C.G. in the x, y, z directions, respectively
b	Blade semi chord
C_{d0}	Blade drag coefficient
C_{m0}	Blade moment coefficient
C_w	Weight coefficient
C_x, C_y, C_z	Blade damping constants

e	Hinge offset
f	Fuselage equivalent flat plate drag area = $\frac{\bar{f}}{2bR}$
FHX, FHY, FHZ	Vibratory hub shears with HHC in the longitudinal, lateral and vertical directions, respectively
FHXb, FHYb, FHZb	Baseline vibratory hub shears in longitudinal, lateral and vertical directions, respectively
I_b	Blade flap inertia about hinge
$I_{C_{xx}}, I_{C_{yy}}, I_{C_{zz}}$ $I_{C_{xy}}, I_{C_{yz}}, I_{C_{xz}}$	Fuselage mass moments and products of inertia about the fuselage center of mass
J_x	Blade inertia about the feathering axis
K_x, K_y, K_z	Blade spring constants
\bar{M}_B	Dimensional blade mass
M_F	Fuselage mass
N_b	Number of blades
q_b, q_f, q_e, q_t	Vector of the degrees of freedom of blade, fuselage rigid body modes, fuselage elastic modes and trim variables
q_{b0}, q_{bnc}, q_{bns}	Harmonic components of blade response
q_{f0}, q_{fnc}, q_{fns}	Harmonic components of fuselage rigid body response
q_{e0}, q_{enc}, q_{ens}	Harmonic components of fuselage elastic response
\bar{R}	Dimensional rotor radius
R_c	Elastic coupling coefficient
\bar{R}_H	Position vector of hub
R_{Mx}, R_{My}, R_{Mz}	Translational degrees of freedom of C.G of the helicopter

[i] Ph.D. Candidate

[ii] Associate Research Engineer

[iii] Professor and Chairman

T, T_{AF}, T_{FA}	HHC Transfer matrices	$\vec{\omega}$	Vector of angular velocity
U, V, W	Blade displacements	$\vec{\omega}_H$	Vector of angular velocity at hub due to fuselage motion
X	Position along the blade from the hinge offset point	$\omega_{BV1}, \omega_{BH1}, \omega_{T1}$	Fundamental fuselage natural frequencies in vertical bending, horizontal bending and torsion
X_{Ma}, Z_{Ma}	X and Z position of the fuselage aerodynamic center from point M on the helicopter	$\omega_{BV2}, \omega_{BH2}, \omega_{T2}$	Second fuselage natural frequencies in vertical bending, horizontal bending and torsion
X_{MC}, Z_{MC}	X and Z position of the fuselage center of mass from point M on the helicopter	$\omega_{F1}, \omega_{L1}, \omega_{T1}$	Rotating first flap, lag, and torsional blade frequencies
X_{MH}, Z_{MH}	X and Z position of the rotor hub center from point M on the helicopter	$\bar{\omega}_{HH}$	Frequency of the HHC input
Y_o, Z_o	Y and Z position of the point "p" on the cross section of the blade	Ω	Rotor R.P.M
		$(\bar{\quad})$	Overbars indicate dimensional quantities
Z, Z_A, Z_F	Vectors of vibratory response		
Z_0	Vector of baseline vibrations		
α_R	Fuselage attitude in pitch		
β_k, ζ_k, ϕ_k	The k-th blade rotating flap, lead-lag and torsional degrees of freedom		
γ	Lock number		
$\theta_0, \theta_{1c}, \theta_{1s}$	Blade pitch settings for equilibrium		
$\theta_T(x_k)$	Blade twist distribution		
θ_G	Total blade pitch angle		
θ_{HHC}	Higher Harmonic Control input		
θ	Vector of HHC inputs		
$\theta_{OH}, \theta_{CH}, \theta_{SH}$	Collective, lateral and longitudinal HHC inputs in the nonrotating frame		
$\theta_x, \theta_y, \theta_z$	Fuselage roll, pitch and yaw degrees of freedom		
λ	Total inflow		
μ	Advance ratio		
ρ_A	air density		
σ	Solidity ratio = $\frac{2N_b b}{\pi}$		
$\phi_{OH}, \phi_{CH}, \phi_{SH}$	Phase angles of collective, lateral and longitudinal HHC inputs		
ϕ_s	Fuselage attitude in roll		
ψ, Ψ	Blade azimuth angle		

Introduction

Vibrations in helicopters are caused by a variety of sources, such as rotor systems, engine, transmission etc.. Vibratory loads lead to fatigue damage of structural components, human discomfort, difficulty in reading instruments and reduced effectiveness of weapon systems. These oscillatory loads are often sensitive to the design parameters of the rotor and fuselage system. Furthermore, these loads increase with advance ratio and depend on flight conditions. With increasing demand for high speed and high maneuverability for both military and civilian applications, vibration analysis of helicopters plays a key role in helicopter design. Therefore, during the last decade a substantial amount of research by both industry and academia has been aimed at improving the fundamental understanding of the effect of various blade and fuselage parameters on the vibration levels encountered in coupled rotor-fuselage systems. Excellent reviews on the sources of vibrations in helicopters and a description of the methods for reducing vibration levels were presented by Reichert[1] and Loewy[2].

Traditionally, vibration analysis in helicopters has been performed in two stages. In the first stage, the rotor blade and hub loads are evaluated by rotor load codes representing the complex structural and aerodynamic characteristics of the rotor system. The resulting hub loads are then introduced as forcing functions to either a detailed finite element model of the fuselage or to a ground shake test to estimate the fuselage vibration levels. Often this approach leads to unreliable prediction of vibratory levels in helicopters. By using a simple model of a coupled rotor-fuselage system and following an impedance matching technique, it was shown by Staley and Sciarra[3] that the hub loads evaluated from a fixed hub condition cannot be applied as direct forcing functions to a fuselage since such a procedure does not adequately represent the coupled rotor-fuselage system dynamics. The principal reason for this inaccuracy is due to the fact that fuselage motions cause the hub to translate and rotate which in turn modifies the hub loads. As an extension of Ref.[3] several studies have been performed using a simple coupled rotor-fuselage model and impedance matching techniques. In Ref. [4] it was shown that by tuning the fuselage natural frequency to the blade passage frequency, it is possible to eliminate the hub loads.

However Hsu and Peters[5] concluded that such a reduction in hub loads does not necessarily mean a reduction in the fuselage vibratory response. Furthermore, it is shown that the fuselage vibratory motion and hub loads are sensitive to the placement of the fuselage and blade natural frequencies. This conclusion was obtained using impedance matching techniques in Ref. [5] and [6], with a simple finite element representation of the fuselage in a coupled rotor-fuselage model in Ref.[7] and with a fully coupled linear rotor-fuselage model in Ref. [8]. These studies illustrate the significance of rotor-fuselage coupling in the vibration analysis of helicopters. However it is important to recognize that most of these studies were based on linear mathematical models for the coupled rotor-fuselage dynamic system. These linear models use only flapping motion of the blade and a rigid fuselage with a spring restraint between the fuselage and the rotor hub. An exception is Ref.[7] where the fuselage was modelled as an elastic beam, however the blade model was restricted to one having flapping motion only and the vibratory loads considered were the vertical hub shears; shears in the hub plane and the hub moments were neglected. While these studies represent significant contribution toward the understanding of the mechanism of helicopter vibration, they do not include some important effects, such as: lag and torsional deformation of the rotor blades, the nonlinear gyroscopic and other coupling terms involving the rotor-fuselage degrees of freedom, the elastic modes of the fuselage in addition to the rigid body modes. Realizing the need for a general nonlinear mathematical model, Kunz [9] and Venkatesan and Friedmann[10,11] have developed a nonlinear mathematical model for a coupled rotor-fuselage dynamic system. Only limited numerical results were presented in Ref.[9] while Refs.[10,11] were aimed at the study of aeromechanical stability problems in a coupled rotor-fuselage system.

Intimately linked to the problem of vibration prediction is the problem of vibration reduction in helicopters. Among the various schemes available for vibration reduction [1,2] vibration reduction using higher harmonic control (HHC) appears to have considerable promise. Vibration reduction using HHC has been demonstrated by analytical simulation [12-17], wind tunnel tests [18-21] and flight tests [22-24]. The analytical studies and wind tunnel tests have shown that under a fixed hub condition, the use of high frequency blade pitch inputs (HHC) reduces hub loads. These studies essentially assume that a reduction of hub shears is equivalent to reducing the vibrations in the flexible fuselage. It should be noted that the purpose of the analytical and wind tunnel studies was not only to assess the effectiveness of various control algorithms for HHC but also to demonstrate the technical feasibility of the approach. On the other hand, flight tests have demonstrated fuselage vibration (usually acceleration levels at the pilot seat) reduction by using HHC inputs to the main rotor. In some flight tests it was observed that reduction of acceleration components at the pilot seat was accompanied by increases in hub and blade loads from their baseline values. In flight fuselage vibrations are caused by a combination of many sources in addition to the main rotor, such as tail rotor, transmission, rotor fuselage aerodynamic interactions, the engines etc.. Furthermore fuselage vibration characteristics are significantly influenced by the complex structural dynamic behavior of the flexible fuselage. Therefore vibration reduction by HHC in a flight test can be interpreted as

using the main rotor as an active vibration absorber, which cancels vibrations in the fuselage by modifying the unsteady aerodynamic, elastic and inertial loads on the rotor. Thus a number of fundamental questions pertaining to vibration reduction using HHC can be posed, such as :

- (1) Is vibration reduction at the hub, using HHC, equivalent to vibration reduction at a particular location in the fuselage (pilot seat) ?
- (2) What is the influence of the fuselage flexibility on the vibration reduction schemes ?

To provide answers to these questions, one has to develop a consistent nonlinear mathematical model for the coupled rotor-flexible fuselage dynamic system in forward flight. Experience has shown that the derivation of the mathematical model for the coupled rotor-fuselage system becomes quite complex and algebraically tedious due to the presence of a large number of terms representing the dynamic and aerodynamic loads. Therefore, the development of a nonlinear mathematical model, representing the coupled rotor-fuselage dynamic system, by computer algebra is significant because it relegates these tedious tasks to the computer. Only a limited number of papers were published on computerized symbolic derivation of dynamic equations of motion for helicopters. Automatic generation of these equations, based on an explicit formulation using a special purpose symbolic manipulator written in FORTRAN was first done by Nagabhushanam et al. [25]. These equations were further refined and combined with numerical techniques to perform aeroelastic calculations for hingeless rotor blades in forward flight [26]. Another approach was to use commercially available symbolic manipulation packages, such as REDUCE or MACSYMA to generate the explicit nonlinear equations of motion. The methodology of deriving flexible blade equations using MACSYMA on a dedicated LISP computer is discussed in ref. [27].

The main objectives of this study are :

1. To demonstrate the symbolic derivation of the nonlinear equations of a coupled rotor-flexible fuselage dynamic system in forward flight, using a symbolic computing facility.
2. To determine whether reduction in hub shears by HHC is equivalent to reducing the fuselage vibration levels at a particular location in the fuselage and vice versa.
3. To determine the influence of the fuselage flexibility and modal characteristics of the fuselage [30] on the vibratory response of the coupled rotor-fuselage system.
4. To explore the feasibility of the simultaneous reduction of both the hub loads and the fuselage accelerations at any location, for example the C.G.. This is accomplished by a modified scheme for HHC denoted in this paper by the expression " Multiple Higher Harmonic Control " (MHC).

Coupled Rotor/Fuselage Model

The first step in studying the vibration problem in helicopters is the formulation of the nonlinear differential equations of motion representing the dynamics of the coupled rotor-flexible fuselage system in forward flight. Due to the complexity of the problem, certain simplifying assumptions have been made in the idealization of the rotor-fuselage system, as shown in Fig. 1 . In this model, the rotor blades are idealized as

rigid blades with three orthogonal root springs representing the flexibility of the blade in the flap, lag and torsion respectively. The fuselage is idealized as a uniform beam having bending deformations in the vertical and horizontal planes and elastic torsion about the \hat{x}_1 axis. In addition to the elastic deformations, the fuselage has five rigid body degrees of freedom namely, pitch, roll and three translations. The rotor system is connected to the flexible beam through a rigid shaft at point "D".

The equations of motion of the coupled rotor-flexible fuselage system are derived using force and moment equilibrium conditions. The rotor blade equations are obtained by enforcing moment equilibrium at the root of the blade; the rigid body equations of motion of the fuselage are obtained using force and moment equilibrium at the C.G. of the fuselage; and the elastic mode equations of the fuselage are formulated using generalized force and moment equilibrium in various generalized modes representing the elastic deformation of the fuselage.

The final equations contain a provision for incorporating HHC type of pitch inputs. These pitch inputs, in the rotating frame, are represented by:

$$\begin{aligned} \theta_{\text{HHC}} = & [\theta_{\text{OH}} \sin(\bar{\omega}_{\text{HH}}\psi + \phi_{\text{OH}})] \\ & + [\theta_{\text{CH}} \sin(\bar{\omega}_{\text{HH}}\psi + \phi_{\text{CH}})] \cos \psi \\ & + [\theta_{\text{SH}} \sin(\bar{\omega}_{\text{HH}}\psi + \phi_{\text{SH}})] \sin \psi \end{aligned} \quad (1)$$

Using this pitch input the influence of HHC on the vibration levels of the coupled rotor-fuselage system in forward flight is studied in detail.

Symbolic Manipulation

The nonlinear equations of motion representing the dynamics of the coupled rotor-fuselage system were derived using a special purpose symbolic computing facility consisting of a Symbolics 3650 machine equipped with the MACSYMA symbolic manipulation program, and networked with a SUN 3/280 computer on which the numerical computations are carried out. The symbolic manipulation program MACSYMA is used to generate the mathematical expressions of the equations of motion, in a format suitable for their incorporation in the FORTRAN code needed to perform the numerical computations. A brief description of the methodology employed in formulating the equations of motion using symbolic manipulation together with the basic features of such a scheme are provided below.

The MACSYMA commands that appear in this paper and their detailed description can be found in the MACSYMA Reference manual [28]. The various steps followed sequentially in the derivation of the equations of motion and the associated algebraic manipulations can be classified as follows:

1. Definitions
2. Algebraic manipulations
3. Conversion to FORTRAN format

(1) Definitions: Initially, all the system degrees of freedom such as blade flap-lag-torsional deformations, fuselage rigid body motions and elastic deformations, along with their functional dependencies on time (PSI) and space (X) variables are defined, by using the MACSYMA command "DEPENDS". For example, the expression

DEPENDS ([U,V,W, ...], PSI, [U,V,W, ...], X) \$

defines that the variables U, V, W, ... depend on the nondimensional time (PSI) and the space variable (X) along the blade span.

In the next step, the coordinate transformation matrices between the various rotating and nonrotating, deformed and undeformed coordinate systems are defined. For example, the transformation between the hub fixed rotating and nonrotating coordinate systems is defined by using the command

```
T21 : MATRIX ([ COS(PSI), SIN(PSI), 0 ],
              [ -SIN(PSI), COS(PSI), 0 ],
              [ 0, 0, 1 ]) $
```

This statement provides the coordinate transformation of a vector expressed in the hub fixed nonrotating system "1" to the hub fixed rotating system "2k":

$$\{ \}^{2k} = [T21] \{ \}^1$$

It must be pointed out that for the present coupled rotor-fuselage vibration analysis, 9 different coordinate systems were used. The matrices corresponding to the transformations between these coordinate systems are all defined in this first stage of the formulation of the equations of motion.

The assignment of the order of magnitude to the various quantities was performed using the MACSYMA command

```
RATWEIGHT ( VAR1, I1, VAR2, I2, ... ) $
```

where VAR₁, VAR₂, ... represent quantities, such as U, V, W, ... and I₁, I₂, ... define the orders of magnitude of those quantities. It is important to point out that MACSYMA can only handle integer values (0,1,2,3, ...) for the order of magnitude. In the present formulation, the fuselage motions have been defined to be of the order O($\epsilon^{3/2}$). This order of magnitude for the fuselage motions is proved to be fairly accurate in capturing the essential features of the rotor-fuselage coupling [29]. To incorporate the definition of O($\epsilon^{3/2}$), in the present analysis, the orders of magnitude of all the quantities are multiplied by a factor of 2, so that in the symbolic manipulation program, only integer numbers appear as orders of magnitude. Based on these modified orders of magnitude definitions of the various quantities, the implementation of the ordering scheme

$$1 + O(\epsilon^2) \approx 1 \quad (2)$$

which states that terms of order ϵ^2 are negligible relative to terms of order unity was also modified in the symbolic manipulator program to

$$1 + O(\epsilon^4) \approx 1 \quad (3)$$

which states that terms of order ϵ^4 are negligible relative to terms of order unity. The quantity ϵ is a small non-dimensional parameter, chosen to define what a "small" term is. In the context of this research ϵ is equal to the blade slopes in flap and lag, which for the offset hinged restrained blade model are equivalent to the flap and lag angles of the blade. To systematically eliminate the

higher order nonlinear terms the MACSYMA command

RATWTLVL : n \$

is used to set the "rational weight level" to n, which causes the terms whose order of magnitude is greater than $O(\epsilon^n)$ to be deleted.

In addition, the position vector \vec{R}_p of a material point "p" on the cross-section of the deformed blade and the angular velocity vector $\vec{\omega}$ are defined as :

$$\vec{R}_p = \vec{R}_H + e \hat{x}_2 + (X + U) \hat{x}_3 + V \hat{y}_3 + W \hat{z}_3 + Y_o \hat{y}_4 + Z_o \hat{z}_4 \quad (4)$$

and

$$\vec{\omega} = \vec{\omega}_H + \Omega \hat{z}_1 \quad (5)$$

The first terms on the right hand side of Eqs. (4) and (5) represent the contribution of the hub motion. The second term in Eq. (5) represents the blade rotation at a constant angular speed. The unit vectors in equations (4) and (5) are associated with the coordinate systems described below. The "1" system is body fixed to the fuselage with its origin located at the hub center. The unit vector \hat{z}_1 always points upward along the rotor shaft and \hat{x}_1 and \hat{y}_1 point to the rear and to the pilot's right side. The "2" or "2k" system can be defined by taking the "1" system and rotating it around the shaft axis so that the \hat{x}_2 axis is rotating with the k-th blade. The "3" system is tilted by a constant precone angle β_p from the "2" system so that the unit vector \hat{y}_3 points in the same direction as \hat{y}_2 . The "4" system is fixed in a cross section of the rotating blade. Since we are using the offset hinged spring restrained approximation for a hingeless blade, the "4" system is attached to the blade so that \hat{x}_4 is along the length of the blade and it coincides with the elastic axis of the hingeless blade. The coordinate transformation from "3" to "4" follows the sequence of flap-lag-torsion type of blade deformation. All these definitions are stored in a MACSYMA program module which is executed in batch mode to create the environment for the next stage, the algebraic manipulation, in order to obtain the inertial and aerodynamic loads. An additional advantage of this modular approach consists of the ability to select any ordering scheme and thereby retain nonlinear terms up to any desired order.

(2) Algebraic manipulation: Using the definitions of the position vector of a material point and the angular velocity vector, the necessary differentiations and the associated algebraic, matrix and trigonometric manipulations are performed symbolically to obtain the expressions for the velocity and acceleration components of the material point. The symbolic differentiation is performed by the MACSYMA command

DIFF(FUNC, VAR, n) \$

which evaluates the nth order derivative expression of function FUNC with respect to the variable VAR. Based on D' Alembert's principle, the inertial forces per unit volume and the inertial moments per unit volume

about the elastic axis at the location of the typical cross-section of the blade are formulated. Performing an integration over the cross-section, the distributed inertial loads per unit span of the rotor blade are obtained. In this step the cross-sectional inertia properties (I_{MB2}, I_{MB3}, X_I) are essentially substituted for the appropriate integrals via the MACSYMA command

RATSUBST(A, B, EXP) \$

which substitutes A for B in expression EXP.

Next, using the aerodynamic load expressions (based on Greenberg's theory with quasi-steady assumption) and the velocity components at various cross-sections of the blade, the distributed aerodynamic blade loads per unit span are formulated.

In the load expressions, obtained in this manner by MACSYMA, standard mathematical operators, such as

$$\frac{d(\)}{d\psi}, \frac{d(\)}{dx},$$

powers, divisions, matrix forms are displayed in a visually comprehensive format that is not in a form readable by MACSYMA. In order to save the various load expressions in a form which is suitable for further manipulations with MACSYMA, the command "GRIND" combined with "WRITEFILE" and "CLOSEFILE" is used as shown below.

WRITEFILE("FILENAME");

GRIND(LOAD1);

GRIND(LOAD2);

.

CLOSEFILE();

The sequence of MACSYMA commands, presented above, saves the MACSYMA readable display of load expressions, produced by the commands "GRIND", in the file FILENAME (which is automatically created by MACSYMA in the LISP machine file system and saved as soon as "CLOSEFILE" is reached).

(3) Conversion to FORTRAN: The various inertia and aerodynamic load expressions have to be converted to a form suitable for FORTRAN coding. This translation is performed in two steps. In the first step, the differential and trigonometric expressions are substituted by FORTRAN compatible variable names. Next, using the MACSYMA command "FORTRAN" combined with "WRITEFILE" and "CLOSEFILE", the load expressions are stored after being converted to FORTRAN readable statements. The files containing these statements are then transferred to the SUN 3/280 through the network and incorporated in the FORTRAN 77 code which is used to obtain the numerical results. It is important to note that all the differentiations, integrations, coordinate transformations and associated algebraic manipulations are performed using the symbolic manipulator, thereby substantially reducing the time involved in formulating the equations and reducing the potential for human error.

Method of solution

The procedure used for calculating the equilibrium state and the vibratory loads on the helicopter is based

on a harmonic balance technique. In Ref.[31], different methods of solving the coupled rotor-fuselage problem are discussed. Usually, the trim state representing the equilibrium condition of the helicopter is solved separately from the response problem. When following this approach, only the flapping blade degree of freedom is considered in evaluating the equilibrium state of the helicopter. In this study, the trim state of the helicopter and the response solution are obtained in a single pass by simultaneously satisfying the trim equilibrium and the vibratory response of the helicopter for all the rotor and fuselage degrees of freedom. This is an extension of the method developed for aeromechanical stability control problem, in Refs 32 and 33. For the sake of clarity a brief description of the method is provided below. The equations of motion for the coupled rotor-flexible fuselage system can be symbolically written as:

$$f_b(q, \dot{q}, \ddot{q}, q_t; \psi) = 0 \quad (6)$$

$$f_f(q, \dot{q}, \ddot{q}, q_t; \psi) = 0 \quad (7)$$

$$f_e(q, \dot{q}, \ddot{q}, q_t; \psi) = 0 \quad (8)$$

$$f_\lambda(q, \dot{q}, \ddot{q}, q_t; \psi) = 0 \quad (9)$$

The vector f_b represents the flap,lag and torsional blade equations. The vector f_f represents the fuselage rigid body motion equations. The vector f_e represents the fuselage elastic deformation equations. Finally, f_λ represents the inflow equation. The trim solution is the vector q_t , representing the quantities λ , θ_0 , θ_{1c} , θ_{1s} , α_R , and ϕ_s . The response solution represented by q , consists of the following :

$$q = \begin{bmatrix} q_b \\ q_f \\ q_e \end{bmatrix} \quad (10)$$

The vector q_b contains the blade degrees of freedom β_k , ζ_k , and ϕ_k . The vector q_f consists of the five fuselage degrees of freedom R_{Mx} , R_{My} , R_{Mz} , θ_x , θ_y . The fuselage yaw degree of freedom is not considered in the present analysis. The vector q_e represents the generalized displacements ξ_i of the fuselage elastic modes. In forward flight a periodic solution in the form of Fourier series is assumed:

$$q_b = q_{b0} + \sum_{n=1}^{N_{Hb}} q_{bnc} \cos n\psi_k + q_{bns} \sin n\psi_k \quad (11)$$

$$q_f = q_{f0} + \sum_{n=1}^{N_{Hf}} q_{fnc} \cos nN_b\psi + q_{fns} \sin nN_b\psi \quad (12)$$

$$q_e = q_{e0} + \sum_{n=1}^{N_{He}} q_{enc} \cos nN_b\psi + q_{ens} \sin nN_b\psi \quad (13)$$

where N_{Hb} , N_{Hf} , N_{He} represent the number of harmonics for the blade, fuselage rigid body and fuselage elastic mode response, respectively.

It is known that only those components of the loads that are integer multiples of the rotor passage frequency $n \times N_b$ will be transmitted to the fuselage through the rotor hub. Hence the response of the fuselage rigid body and elastic degrees of freedom contains only integer multiples of N_b per rev harmonics. The vibratory response of the fuselage rigid body degrees of freedom was evaluated about an equilibrium state. Hence the constant pitch and roll attitudes of the fuselage are not included in the response expressions and they appear only in the trim vector q_t . The substitution of equations Eqs. (11) - (13) in equations Eqs. (6) - (9) combined with the harmonic balance technique yields a system of nonlinear coupled algebraic equations. Solution of the nonlinear algebraic system is obtained using a Newton algorithm.

The global model of the helicopter response to HHC assumes linearity over the entire range of control application:

$$Z = Z_0 + T\theta \quad (14)$$

where θ is the HHC vector, defined as:

$$\theta = \{\theta_{OC} \theta_{OS} \theta_{CC} \theta_{CS} \theta_{SC} \theta_{SS}\}^T \quad (15)$$

The individual components of this vector are the cosine and sine components of the collective, lateral and longitudinal HHC inputs, θ_{OH} , θ_{CH} , θ_{SH} respectively. The vibration vector Z is equal to the baseline vibration Z_0 plus the product of the transfer matrix T and the HHC vector θ

From the solution of the response problem, rotor hub forces and moments and C.G. accelerations are available in three orthogonal directions. Sine and cosine components of the 4/rev. harmonics are also available. Any combination of these quantities can be used as a measure of vibration levels and thus can be selected as the objective which is to be minimized. In this study the cosine and sine components of the 4/rev. hub forces or C.G. accelerations in the longitudinal, lateral and vertical direction are to be minimized. The vector of hub vibratory shears Z_F is defined as:

$$Z_F = \{F_{Hx4c} F_{Hx4s} F_{Hy4c} F_{Hy4s} F_{Hz4c} F_{Hz4s}\}^T \quad (16)$$

The vector of C.G. accelerations Z_A is defined as:

$$Z_A = \{A_{Cx4c} A_{Cx4s} A_{Cy4c} A_{Cy4s} A_{Cz4c} A_{Cz4s}\}^T \quad (17)$$

Equation (14) is used to estimate the transfer matrix, T . The columns of the matrix are formed by using a small HHC input of .005 rad for each component of the vector θ separately (with all the other components set to zero) and calculating the resulting change in the 4/rev components of the hub loads or C.G. accelerations. The HHC input vector is evaluated using the relation:

$$\theta = -[T]^{-1} Z_0 \quad (18)$$

If we decide to minimize Z_F the matrix will be T_{AF} and HHC vector will be θ_{AF} . If we chose to minimize Z_A the matrix will be T_{FA} and HHC vector will be θ_{FA} . The

two inputs are generally different and it is our objective to study how they vary with respect to the fuselage flexibility. It is also important to determine how hub shears and moments change when θ_{FA} is applied and similarly, how C.G. accelerations and hub moments change when θ_{AF} is used.

If all 12 components of the 4/rev harmonics of the hub shears followed by the 4/rev harmonics of the C.G. accelerations are to be simultaneously minimized the vibration vector, Z will be defined as:

$$Z_{FA} = \{Z_F^T \ Z_A^T\}^T \quad (19)$$

The HHC input vector θ will now have 12 components and will be defined as:

$$\theta = \{\theta_p^T \ \theta_q^T\}^T \quad (20)$$

where (p,q) indicate the two HHC frequencies, $\bar{\omega}_{HH}$ applied to the pitch input. The transfer matrix T will now be of size 12×12 and will again be calculated from Eq. (14).

Results and Discussion

The results presented in this section are for a coupled rotor/ fuselage system which has the following degrees of freedom: coupled flap-lag-torsional deformation in each blade of a four bladed rotor system, five rigid body degrees of freedom for the fuselage, and two flexible modes for bending in the vertical plane, bending in the horizontal plane and torsion along the \hat{x}_1 axis, respectively. The final set of equations representing the equilibrium and response of the coupled rotor-fuselage system are nonlinear algebraic equations and the unknowns are the harmonic components of the response and trim settings of the helicopter. Five harmonics were used for the blade response (33 unknowns), one harmonic was used for the fuselage rigid body response (10 unknowns), one harmonic for the fuselage elastic response (18 unknowns) and five trim variables (5 unknowns) were included in the analysis. Thus the total number of unknowns in this model is 66.

The results presented are for an advance ratio of $\mu = 0.3$. The data used is presented in Table 1.

Figures 2 and 3 show the variation of the vibratory hub loads as a function of the fundamental frequency of the fuselage in vertical bending. It can be seen from these figures that when the fundamental frequency of the fuselage is near 1.45/rev or 4/rev the vibratory hub loads exhibit either a peak or a dip. It should be pointed out that when the fundamental frequency is near 1.45/rev, the frequency of the second bending mode of the fuselage is near 4/rev. Therefore, the response characteristics indicate that whenever a fuselage frequency is near 4/rev, a resonance occurs in the response of the hub loads. From Fig. 2, it can be seen that while the longitudinal and lateral vibratory hub shears exhibit a roller-coaster behavior at resonance, the vertical hub shear shows a sharp resonance peak only. Similarly the hub moments in pitch and roll also exhibit a roller-coaster behavior (Fig. 3). Such a behaviour in the response is consistent with the observations made in Refs. [4],[6] and [8].

Figure 4 shows the variation of the acceleration of the C.G. of the fuselage (point C in Fig. 1'). While the longitudinal acceleration shows a roller-coaster behavior near resonance, for this case, the vertical acceleration exhibits only a resonance peak. From the results shown in Figs. 2 through 4, one can conclude that the

resonant behavior of the response occurs over a very narrow range of fuselage frequency.

Next, the effect of introducing open loop HHC pitch variation in collective, lateral cyclic and longitudinal cyclic modes is studied, in order to determine the relative influence of these three control inputs on the vibratory response of the coupled rotor/fuselage system. A preliminary check showed that our assumption about the linearity of the HHC model is valid in the range of 0 to 0.005 rad for $\omega_{BV1} = 4/\text{rev}$ at various fixed phases. This study is performed for three different configurations where the fuselage bending frequency in the vertical plane has different values, namely: (a) rigid fuselage (b) the fundamental frequency of the fuselage in vertical bending is $\omega_{BV1} = 4/\text{rev}$ and (c) the fundamental frequency of the fuselage in vertical bending is $\omega_{BV1} = 1/\text{rev}$. Figures 5 to 7 show the influence of collective, lateral cyclic and longitudinal cyclic HHC inputs on the vibratory hub shears. The results are obtained by keeping the amplitude of the HHC at .005 rad, while the phase is varied from 0° to 360° . In these figures FHXB, FHYB, FHZB refer to the baseline values obtained without HHC inputs and are plotted using the dotted, broken and solid lines, respectively. Similarly, the vibratory hub shears FHX, FHY, FHZ after the application of HHC are represented by the same lines which are marked with the symbol "x", to distinguish them from the baseline case. It can be seen from Fig. 5 that the phase of the collective HHC input has a large influence on the vibratory vertical hub shears when the fuselage frequency in the fundamental mode is $\omega_{BV1} = 1/\text{rev}$ or when the fuselage is rigid. However, it should be noted that in these cases the collective HHC input increases the vibratory hub shears from their baseline values. When the fuselage frequency in the fundamental mode is $\omega_{BV1} = 4/\text{rev}$, the collective HHC input has less influence on the vertical hub shears. Furthermore, collective HHC input has a limited effect on the hub shears in the longitudinal and lateral directions.

Figure 6 shows the influence of lateral HHC input on the vibratory hub shears. In this case, the lateral HHC control input has a large influence on the vertical hub shear for all fuselage frequencies considered. It is important to note from this figure that the lateral control input reduces the vibratory hub shears in the vertical direction and this reduction does not depend on the fuselage frequencies. When the fuselage is rigid or when the fuselage frequency is 1/rev, the vertical hub shear is reduced below the baseline value for the range of phase angles between $240^\circ \sim 360^\circ$. When the fuselage frequency is 4/rev, the phase angle range required for a reduction in vertical hub shears is $150^\circ \sim 300^\circ$.

Figure 7 shows the influence of longitudinal HHC input on the hub shears. The influence of longitudinal HHC input on the vibratory loads is more pronounced when the fuselage is either rigid or has a fundamental frequency of 1/rev. Also, for all fuselage frequencies considered, the longitudinal HHC input reduces the vibratory hub shears.

The influence of HHC inputs on the fuselage accelerations at the C.G. is shown in Figures 8 through 10. In these figures ACXB, ACYB, ACZB refer to the baseline values obtained without using HHC inputs and are plotted using the dotted, broken and solid lines, respectively. Similarly, the vibratory C.G. accelerations ACX, ACY, ACZ after applying HHC are represented by the same lines which are marked with the symbol "x", to distinguish them from the baseline case. Figure

8 shows the influence of collective HHC input on the C.G. acceleration. It can be seen from this figure that when the fuselage is treated as a flexible body, the collective HHC input reduces the vertical C.G. acceleration from the baseline value. When the fuselage is assumed to be a rigid body, collective HHC input increases the vertical C.G. acceleration from the baseline value.

Figure 9 illustrates the influence of lateral HHC input on the C.G. accelerations. It is evident that the lateral HHC input is very effective in reducing the fuselage C.G. accelerations, for all fuselage frequencies considered. A similar observation can be also made for the longitudinal control input shown in Fig. 10

From the results presented in Figs. 5 through 10, one can conclude that the cyclic HHC input is the most effective means for reducing the hub shears or C.G. accelerations for all fuselage frequencies considered. The influence of the collective HHC input in reducing the fuselage C.G. accelerations or hub shears depends on the modelling of the fuselage flexibility (or its frequency). When the fuselage is treated as a rigid body, collective HHC input can actually increase the vibratory hub shears and C.G. accelerations from their baseline values.

Using an open-loop control model, the HHC inputs required to minimize the hub shears or C.G. accelerations were obtained for various fuselage representations. Figure 11 shows the amplitude of the 4/rev hub loads when HHC pitch inputs to the blade are aimed at minimizing C.G. accelerations. When the fuselage is treated as a flexible body and the HHC for minimizing the C.G. accelerations is applied, the fourth harmonic component of the vertical hub shear increases by a factor of six from its baseline value. However when the fuselage is treated as a rigid body, the vertical hub shear is reduced almost to zero. It is also evident from this figure that the inplane hub shears are reduced to zero when HHC inputs are provided. This result indicates that when the fuselage is treated as a flexible structure, a minimization of the C.G. acceleration by HHC increases the vertical hub shear. Whereas when the fuselage is treated as a rigid body, the HHC inputs required to reduce the C.G. acceleration will also reduce the hub shears.

Figure 12 shows the amplitude of the 4/rev harmonics of the C.G. acceleration when the HHC input is aimed at minimizing hub shears. Again it is evident that for a flexible fuselage model, the vertical C.G. acceleration increases by a factor of 3~5 from its the baseline value, when an HHC input aimed at minimizing the hub shears is introduced. On the other hand when the fuselage is treated as a rigid body, a reduction in hub shears and C.G. accelerations occurs simultaneously.

The results shown in Figs. 11 and 12 indicate that in the presence of fuselage flexibility, introduction of HHC inputs aimed at reducing hub shears can cause an increase in the vertical C.G. acceleration. Similarly, introduction of HHC inputs aimed at reducing accelerations at the C.G., causes increases in the vertical hub shears. Simultaneous reduction of both C.G. accelerations and hub shears was observed only when the fuselage was treated as a rigid body. Table 2 shows the HHC pitch angles, in the nonrotating frame, required for minimizing either the hub shears or the fuselage C.G. accelerations for $\omega_{BV1} = 4/\text{rev}$. Figure 13 shows the variation of the pitch angle as experienced by the blade, in the rotating frame. It can be seen that the maximum HHC pitch angle is about $\sim 0.8^\circ$. However the azimuthal

variation of the HHC angle experienced by the blade has fundamentally different characteristics depending on whether the hub shears or the fuselage vibrations are being minimized.

Based on the results presented here, it is evident that a single frequency HHC input (which in this case is 4/rev) was incapable of producing a simultaneous reduction of hub shear and fuselage C.G. accelerations when the fuselage is treated as a flexible body.

In order to reduce the hub loads and C.G. accelerations simultaneously, for the case where the fuselage is treated as a flexible body, a new scheme of HHC is proposed which is denoted by the term "Multiple Higher Harmonic Control" (MHHC). In this scheme, instead of providing a single frequency HHC input (as with the conventional HHC), an HHC input with a combination of two frequencies, such as 3/rev and 4/rev or 3/rev and 5/rev or 4/rev and 5/rev, is applied to the blades in the nonrotating frame.

Before describing the results for the new MHHC scheme for simultaneous reduction of vibratory hub loads and C.G. acceleration levels, it is important to review the method of formulation and solution of this new problem. For conventional HHC input of frequency N_b/rev , superimposed over the trim control inputs, for a N_b bladed rotor system, the control pitch angle experienced by each blade is the same at any given azimuth. Therefore, under the assumption of identical blades and no random excitation, the steady state response of all the blades is identical with the appropriate phase shift of

$$\frac{2\pi}{N_b}(k-1), \quad k = 1, 2, \dots$$

for the k-th blade. Hence, in the formulation of the rotor response problem, a set of flap-lag-torsion equations for only one blade is used. Such a representation, denoted herein as "Single Blade Tracking" (SBT), is usually employed in the aeroelastic stability and response analysis of isolated rotor systems as well as in the solution of coupled rotor/fuselage problems.

By introducing a higher harmonic control input with a frequency other than integer multiples of N_b/rev , the individual blades will no longer have the same control pitch angle at any given azimuth. In this case, even under the assumption of identical blades and no random excitation, the steady state response of the individual blades in the rotor system will not be identical. Therefore, the motion of each blade has to be represented by an independent set of equations and their response should be tracked individually. This type of treatment of the problem is denoted in this paper as "Multi-Blade Tracking" (MBT). Under these conditions, all the harmonics of the rotor loads are transmitted to the fuselage, and hence all the harmonics of the vibratory response of the fuselage rigid body and elastic degrees of freedom have to be included in the analysis.

For the present problem, the total number of unknowns which for the case of single blade tracking is 66 becomes 253 for multi-blade tracking. In this case five harmonics were used for the response of each blade (132 unknowns), five harmonics were used for the fuselage rigid body response (50 unknowns), five harmonics for the fuselage elastic response (66 unknowns) and five trim variables (5 unknowns) were included in the analysis. Due to the large increase in the size of the problem, an approximate treatment with "SBT" and an exact treatment with "MBT" were both investigated, for this

new MHHC scheme. Two sets of results are presented below: set (1) corresponds to "SBT" and set (2) corresponds to "MBT".

(1) Single Blade Tracking: To determine the effectiveness of the MHHC scheme, the worst possible case of the fuselage configuration ($\omega_{BVI} = 4/\text{rev}$) is selected, where the fuselage vibratory C.G. accelerations and hub loads are large. The consequences of applying this improved vibration reduction scheme are illustrated in Fig. 14. In this figure the amplitudes of the hub shears, hub moments and fuselage C.G. accelerations are shown for the baseline case (without HHC) and the cases with MHHC. It can be seen from this figure that by providing MHHC (a superposition of 3/rev and 4/rev or 3/rev and 5/rev HHC inputs), the hub loads (both shears and moments) and C.G. accelerations are reduced simultaneously. It is important to recognize that while this new MHHC scheme was aimed at the reduction of hub shears and C.G. accelerations, the results show that in addition to a hub shears and C.G. accelerations reduction between 600 % ~ 1500 % , the hub moments are also significantly reduced. These results clearly indicate that this approach is potentially very valuable for practical vibration reduction applications.

The MHHC inputs required for the two cases of 3,4/rev and 3,5/rev, are presented in Table 3. In order to assess (a) the feasibility of MHHC and (b) the uniqueness or nonuniqueness of the pitch input requirement for the hub load and vibration reduction scheme, it is important to evaluate the MHHC pitch angle experienced by the blade in the rotating frame.

In figure Fig. 15 the pitch input in the rotating frame is shown for the two cases of MHHC namely the 3,4/rev and 3,5/rev combinations, which are both successful in reducing the hub loads and fuselage accelerations. From this figure it is interesting to note that both 3,4/rev and 3,5/rev combinations of MHHC provide identical pitch angle variations as experienced by the blade in the rotating frame. A fourier analysis of this input indicates that the harmonic content of the MHHC in the rotating system is predominantly 2/rev with a 17% content in 3/rev and a 4% content in 4/rev. This result clearly indicates that there is a unique higher harmonic blade pitch input which reduces the hub loads and fuselage accelerations and it is independent of the higher harmonic input frequency introduced in the nonrotating frame. Furthermore, it is also important to note that the maximum pitch angle requirement for MHHC input is about 1.5° which can be easily implemented in practice. It should be mentioned that the 4,5/rev combination MHHC scheme was not successful in reducing the vibrations and loads simultaneously. The reason for this failure can be easily understood by recognizing that a 4/rev or 5/rev pitch input in the nonrotating frame will not produce the required 2/rev pitch variation in the rotating frame. However the 2/rev pitch variation can be obtained if one of the frequencies of the MHHC scheme is 3/rev .

(2) Multi-Blade Tracking: Using the multi-blade tracking treatment, the uncontrolled baseline vibratory response was calculated and was found to be equal to the baseline response obtained with SBT. In order to determine the effect of MBT on the new MMHC scheme, the MHHC signal (3,4/rev combination) obtained for the SBT case was applied to the rotor system and the resulting vibratory response was computed with MBT. The results of this study are shown in Fig. 16. It

can be seen that the peak-to-peak hub shears, moments and C.G. accelerations are reduced by over 600 % .

In order to check the validity of the new MHHC scheme on a different helicopter configuration, the response problem was solved using the set of rotor/fuselage data, representative of the MBB 105 helicopter, given in Table 4.

In this case, the solution was obtained using multi-blade tracking. The results of the analysis are shown in Fig. 17. From these results, it is evident that the vibratory hub loads and C.G. accelerations were again drastically reduced from their baseline values, with an exception of the rolling hub moment which increased by 70 % . The MHHC signal for this case is shown in Fig. 18, which again indicates the predominance of the 2/rev content in the rotating frame.

The physical explanation for the large 2/rev component in the higher harmonic input pitch angle variation, in the rotating frame, can be explained by analyzing the influence of the control pitch input on the aerodynamic loads of the blade. The principal term in the blade aerodynamic loads for the case of forward flight is proportional to $\mu^2 \sin^2 \psi_k \theta_G$, where θ_G represents the total sectional blade pitch angle due to the control pitch setting (for trim), the HHC pitch input, elastic twist and built in twist. Since $\sin^2 \psi_k$ can be replaced by $0.5(1 - \cos 2\psi_k)$, it can be seen that a 2/rev pitch variation in θ_G will directly influence the 4/rev blade loads. Using conventional higher harmonic control with a 4/rev input, in the nonrotating frame, for a 4 bladed rotor, the pitch input variation in the rotating frame is restricted to 3,4 and 5/rev harmonics only. On the other hand, using MHHC with 3,4/rev or 3,5/rev combination of control inputs in the nonrotating frame, the pitch variation in the rotating frame contains the key 2/rev harmonic, in addition to other higher harmonics. Therefore, the 4/rev blade loads are adjusted by using the principal aerodynamic term, $\mu^2 \sin^2 \psi_k \theta_G$, with 2/rev variation in θ_G .

Concluding Remarks

The equations of motion representing the dynamics of a coupled rotor/flexible fuselage model were derived using a symbolic computing facility. These equations were used to study the vibratory behaviour of a model helicopter so as to develop an improved fundamental understanding of this coupled rotor-fuselage system. Furthermore, the model was also used to assess the effectiveness of various HHC pitch inputs for reducing vibrations at the hub or at specific locations on the flexible fuselage. The most important conclusions obtained in the course of this study are summarized below:

(1) Use of a symbolic computing facility based on MACSYMA is an effective means for deriving mathematical models capable of modeling coupled rotor-fuselage vibration problems.

(2) Examination of the characteristics of the vibratory response at the hub and fuselage reveals that when the fuselage frequency is near 4/rev (for a 4 bladed rotor) the vertical hub loads and vertical C.G acceleration exhibit a resonance peak. On the other hand, the other hub shears, hub moments and C.G accelerations in the longitudinal direction show both positive and negative peaks which are denoted by the term " roller-coaster " behaviour.

(3) For all fuselage frequencies considered, the cyclic HHC inputs are the most effective in reducing the hub

shears or C.G accelerations. On the other hand, the influence of collective HHC input in reducing the vibratory response of the vehicle depends on the modeling of the fuselage flexibility.

(4) When the fuselage is treated as a flexible structure, a minimization of the C.G acceleration by HHC results in an increase in vertical hub shear. Similarly, a minimization of the hub shears by HHC produces an increase in the vertical C.G acceleration. However, when the fuselage is treated as a rigid body, a simultaneous reduction of both hub shears and C.G accelerations by HHC is observed.

(5) When the fuselage is treated as a flexible body introduction of a single frequency HHC pitch input (or conventional HHC input) was incapable of producing a simultaneous reduction of both hub shears and fuselage accelerations at the C.G. However when two HHC pitch inputs having different frequencies (MHHC) were introduced, a large simultaneous reduction of both hub loads and fuselage C.G accelerations was obtained. It was shown that for this simultaneous vibration reduction there is a unique higher harmonic pitch angle variation in the rotating frame having predominantly 2/rev content, with 15% ~ 17% content in 3/rev and 3% ~ 5% content in 4/rev. The magnitude of this higher harmonic pitch angle is of the order of 1 to 2 degrees.

(6) The MHHC signal obtained by tracking the response of a single blade (SBT) is a very good approximation that can be successfully used to minimize the vibratory (peak-to-peak) hub loads and fuselage C.G. accelerations. This was shown by applying the signal as input to an exact coupled rotor/fuselage representation where the response of each blade is individually tracked (MBT) and all the harmonics (up to the 5th) for the fuselage response are included in the analysis.

(7) The MHHC scheme for simultaneous reduction of hub shears and fuselage C.G. accelerations was shown to be successful for two different helicopter configurations, indicating that MHHC has tremendous potential for practical vibration reduction in helicopters.

Acknowledgements

This research was funded by NASA Ames Research Center under grant NAG2-477, the useful comments of the grant monitor Dr. S. Jacklin are gratefully acknowledged. We also wish to acknowledge the funding provided by the U.S. Army Research Office (Dr. G. Anderson, monitor), under grant DAA L03-86-G-0109 which enabled us to purchase and develop our symbolic computing facility.

REFERENCES

1. Reichert, G., " Helicopter Vibration Control-A Survey," *Vertica*, Vol 5, No 1, pp 1-20, 1981.
2. Loewy, R.G., "Helicopter Vibrations : A Technological Perspective," *AHS Journal*, Vol. 29, October 1984, pp.4-30.
3. Staley, J.A. and Sciarra, J.J., "Coupled Rotor-Airframe Vibration Prediction Methods," Rotorcraft Dynamics, NASA SP-352, 1974.
4. Hohenemser, K.H., and Yin, S.K., "The Role of Rotor Impedance in the Vibration Analysis of Rotorcraft," Fourth European Powered Lift Aircraft Forum, Stresa, Italy, Sept. 1978.
5. Hsu, T.K. and Peters, D.A., "Coupled Rotor/Airframe Vibration Analysis by a Combined Harmonic Balance, Impedance Matching Method," *AHS Journal*, Vol. 27, No. 1, Jan. 1982, pp. 25-34.
6. Gabel, R. and Sankewitsh, V., "Rotor-Fuselage Coupling by Impedance," 42nd Annual Forum of the American Helicopter Society, Washington D.C, June 1986.
7. Rutkowski, M.J., "Assessment of Rotor-Fuselage Coupling on Vibration Predictions Using a Simple Finite Element Model," *AHS Journal*, Vol. 28, July 1983, pp. 20-25.
8. Kunz, D.L., "Response characteristics of a Linear Rotorcraft Vibration Model," *Journal of Aircraft*, Vol. 19, No. 4, April 1982, pp. 297-303.
9. Kunz, D.L., "A Nonlinear Response Analysis and Solution Method for Rotorcraft Vibration," *AHS Journal*, Jan 1983, pp. 56-62.
10. Venkatesan C., and Friedmann, P., "Aeroelastic Effects in Multi-Rotor Vehicles with Applications to a Heavy-Lift System, Part 1 : Formulation of Equations of Motion," NASA-CR 3822, August 1984.
11. Venkatesan C., and Friedmann, P., "Aeroelastic Effects in Multi-Rotor Vehicles, Part 2 : Method of solution and Results Illustrating Coupled Rotor-Fuselage Aeromechanical Stability," NASA-CR 4009, 1986.
12. Taylor, R.B., Farrar, F.A., and Miao, W., " An Active Control System for Helicopter Vibration Reduction by Higher Harmonic Pitch," AIAA paper No. 80-0672, 36th AHS Forum, Washington D.C., May 1980.
13. Molusis, J.A., " The Importance of Nonlinearity on the Higher Harmonic Control of Helicopter Vibration," 39th AHS Forum, St. Louis, Missouri, May 1983.
14. Chopra, I., and J.L. McCloud, "A Numerical Simulation Study of Open-Loop, Closed-Loop and Adaptive Multicyclic Control Systems," *AHS Journal*, Vol. 28, No. 1, January 1983, pp. 63-77.
15. Robinson, L., and Friedmann, P.P., " Analytic Simulation of Higher Harmonic Control Using a New Aeroelastic Model," Proc. 30th Structures, Structural Dynamics and Materials Conference, Mobile, Alabama, April 1989. AIAA Paper No. 89.1321.
16. Robinson, L., and Friedmann, P.P., " A Study of fundamental Issues in Higher Harmonic

- Control Using Aeroelastic Simulation," Proc. of National Specialists Meeting on Rotorcraft Dynamics of the American Helicopter Society, November 13-14, 1989, Arlington, Texas.
17. Nguyen, K. and Chopra, I., "Application of Higher Harmonic Control (HHC) to Rotors Operating at High Speed and Maneuvering Flight," Proceedings of the 45th Annual Forum of the American Helicopter Society, Boston, MA, May 1989, pp 81-96.
 18. Molusis, J.A., Hammond, C.E., and Cline, J.H., "A Unified Approach to the Optimal Design of Adaptive and Gain Scheduled Controllers to Achieve Minimum Helicopter Vibration," AHS Journal , Vol.28, no.2, April 1983, pp. 9-18.
 19. Lehmann, G., " The Effect of Higher Harmonic Control (HHC) on a Four-Bladed Hingeless Model Rotor," Vertica , Vol.9, No.3, 1985, pp. 273-284.
 20. Shaw, J., Albion, A., Hanker, E.J., and Teal, R., "Higher Harmonic Control: Wind Tunnel Demonstration of Fully Effective Vibratory Hub Force Suppression," AHS Journal , Vol.34, no.1, January 1989, pp. 14-25.
 21. Ham, N., "Helicopter Individual-Blade-Control and its Applications," 39th AHS Forum, St. Louis, Missouri, May 1983.
 22. Wood, E.R., Powers, J.H., Cline, J.H., and Hammond, C.E., "On Developing and Flight Testing a Higher Harmonic Control System," AHS Journal , Vol.30, no.1, January 1985, pp. 3-20.
 23. Miao, W., and Frye, H.M., "Flight Demonstration of Higher Harmonic Control (HHC) on S-76," 42nd AHS Forum, Washington, D.C., June 1986.
 24. Polychroniadis, M., and Achache, M., "Higher Harmonic Control: Flight Tests of an Experimental System on SA 349 Research Gazelle," 42nd AHS Forum, Washington, D.C., June 1986.
 25. Nagabhushanam, J., Gaonker, G. and Reddy, T. S. R., " Automatic Generation of Equations for Rotor-body Systems with Dynamic Inflow for a Priori Ordering Schemes," Proceedings of the 7th European Rotorcraft forum, Garmisch-Partenkirchen, F.R.G., 1981.
 26. Reddy, T.S.R., and Warmbrodt, W., "Forward Flight Aeroelastic Stability from Symbolically Generated Equations," Journal of the American Helicopter Society , Vol. 31, No. 3, July, 1986, pp.35-44.
 27. Crespo Da Silva, M. R. M. and Hodges, D. H., "The Role of Computerized Symbolic Manipulations in Rotorcraft Dynamic Analysis," Computer and Mathematics with Application , 12A, pp. 161-172, 1986.
 28. MACSYMA Reference manual , Symbolics Inc., June 1986.
 29. Friedmann, P.P. and Venkatesan, C., "Coupled rotor/body aeromechanical stability comparison of theoretical and experimental results," Journal of Aircraft , Vol. 22, No. 2, Feb 1985, pp. 148-155
 30. Stoppel, J. and Degener, "Investigations of Helicopter Structural Dynamics and a Comparison with Ground Vibration Tests," AHS Journal , Vol. 27, April 1982, pp. 34-42.
 31. Stephens, W.B. and Peters, D.A., "Rotor-Body Coupling Revisited," AHS Journal , Vol. 32, No. 1, Jan 1987, pp. 68-72.
 32. Takahashi, M.D. and Friedmann, P.P., " Active Control of Helicopter Helicopter Air Resonance in Hover and Forward Flight," AIAA Paper 88-2407-CP, Proceedings AIAA/ASME/ASCE/AHS 29th Structures, Structural Dynamics and Material Conference, Williamsburg VA, April 1988, pp 1521-1532.
 33. Takahashi, M.D., " Active Control of Helicopter Aeromechanical and Aeroelastic Instabilities," Ph.D. Dissertation, Mechanical Aerospace and Nuclear Engineering Department, University of California, Los Angeles, June 1988.

TABLE 1

Data for the full coupled rotor/fuselage model with flap-lag -torsion dynamics in free flight condition.

Characteristic Dimensions

$$\begin{aligned} \bar{M}_B &= 52 \text{ kg} \\ \bar{\Omega} &= 425 \text{ RPM} \\ \bar{R} &= 6.812 \text{ m} \end{aligned}$$

Rotor Data

$\mu = \text{variable}$	$a = 5.7$
$R_c = 0.0$	$C_{d0} = .01$
$\bar{x}_b = 3.406 \text{ m}$	$\bar{b} = .1337 \text{ m}$
$\bar{I}_b = 804.3 \text{ m}^2 \text{ kg}$	$N_b = 4$
$\bar{J}_x = .241 \text{ m}^2 \text{ Kg}$	$\theta_T = 0 \text{ rad}$
$\omega_{Fl} = 1.15$	$\bar{C}_x = 0.0 \text{ N-m-sec}$
$\omega_{Ll} = 0.57$	$\bar{C}_y = 0.0 \text{ N-m-sec}$
$\omega_{Tl} = 4.5$	$\bar{C}_z = 0.0 \text{ N-m-sec}$
$\bar{\rho}_A = 1.23 \text{ kg/m}^3$	$\gamma = 5$
$C_{m0} = -.02$	$\sigma = .05$

Fuselage Data

$M_F = 8363 \text{ kg}$	$C_w = 0.005$
$\bar{X}_{MH} = 1.333 \text{ m}$	$\bar{X}_{MC} = 1.533 \text{ m}$
$\bar{Z}_{MH} = 1.3624 \text{ m}$	$\bar{Z}_{MC} = 0.00 \text{ m}$
$\bar{X}_{MA} = 1.333 \text{ m}$	$\bar{f} = 1.44 \text{ m}^2$
$\bar{Z}_{MA} = 0.0 \text{ m}$	
$\bar{I}_{Cxx} = 1248 \text{ m}^2 \text{ kg}$	
$\bar{I}_{Cyy} = 4994 \text{ m}^2 \text{ kg}$	

TABLE 2

HHC inputs to minimize the hub shears or the c.g. accelerations (rad).

case	component	HHC input for min. c.g. accelerations		HHC input for min. hub shears	
		cosine	sine	cosine	sine
4/rev	Collective	0.002	0.006	-0.014	-0.002
	Lateral	-0.004	0.0	-0.001	0.001
	Longitudinal	0.002	-0.008	0.0	-0.004

TABLE 3

MHHC inputs for load and vibration minimization (angles in rad).

case	component	3/rev		4/rev	
		cosine	sine	cosine	sine
3/rev, 4/rev comb.	Collective	-0.062	0.046	-0.009	0.029
	Lateral	-0.007	-0.036	0.060	-0.045
	Longitudinal	-0.021	-0.026	0.045	0.059

case	component	3/rev		5/rev	
		cosine	sine	cosine	sine
3/rev, 5/rev comb.	Collective	-0.003	0.001	0.0	0.0
	Lateral	-0.023	0.005	0.007	-0.014
	Longitudinal	0.022	-0.008	0.012	0.009

TABLE 4

Data, representative of the MBB 105 helicopter with flap-lag -torsion dynamics in free flight condition.

Characteristic Dimensions

$\bar{M}_B = 52 \text{ kg}$
 $\bar{\Omega} = 425 \text{ RPM}$
 $\bar{R} = 4.9 \text{ m}$

Rotor Data

$\bar{l} = 4.165 \text{ m}$	$\bar{e} = .735 \text{ m}$
$\mu = \text{variable}$	$a = 5.9$
$R_c = 1.0$	$C_{d0} = .01$
$\bar{x}_b = 1.764 \text{ m}$	$\bar{b} = .1347 \text{ m}$
$\bar{I}_b = 224.7 \text{ m}^2 \text{ kg}$	$N_b = 4$
$J_x = .1873 \text{ m}^2 \text{ Kg}$	$\theta_T = 0 \text{ rad}$
$\omega_{Fl} = 1.15$	$\bar{C}_x = 0.2357 \text{ N-m-sec}$
$\omega_{Ll} = 0.62$	$\bar{C}_y = 14.96 \text{ N-m-sec}$
$\omega_{Tl} = 3.0$	$\bar{C}_z = 29.05 \text{ N-m-sec}$
$\bar{\rho}_A = 1.23 \text{ kg/m}^3$	$\gamma = 5$
$C_{m0} = -.02$	$\sigma = .05$

Fuselage Data

$\bar{M}_F = 1664 \text{ kg}$	$C_w = 0.0042$
$\bar{X}_{MH} = 0.96 \text{ m}$	$\bar{X}_{MC} = 0.96 \text{ m}$
$\bar{Z}_{MH} = 1.1437 \text{ m}$	$\bar{Z}_{MC} = 0.00 \text{ m}$
$\bar{X}_{MA} = 0.96 \text{ m}$	$\bar{f} = 0.79 \text{ m}^2$
$\bar{Z}_{MA} = 0.0 \text{ m}$	
$I_{Cxx} = 1248 \text{ m}^2 \text{ kg}$	
$I_{Cyy} = 4994 \text{ m}^2 \text{ kg}$	

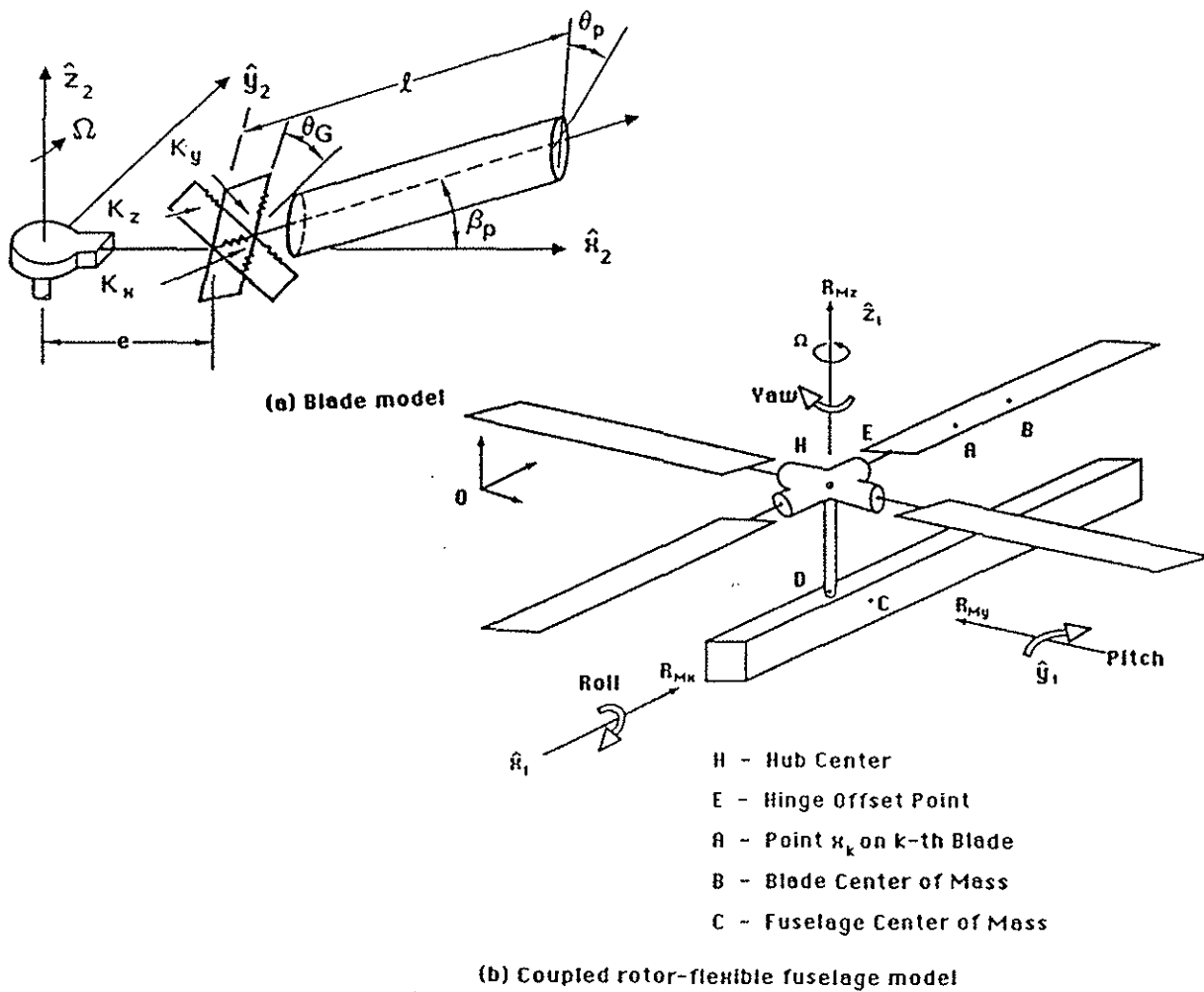


Figure 1: Idealization of the coupled rotor-fuselage system

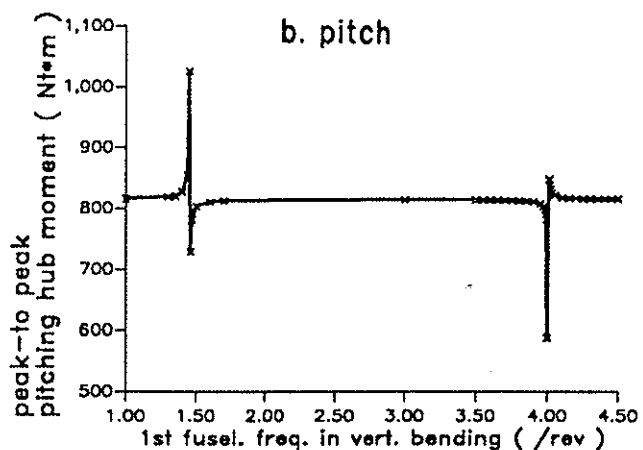
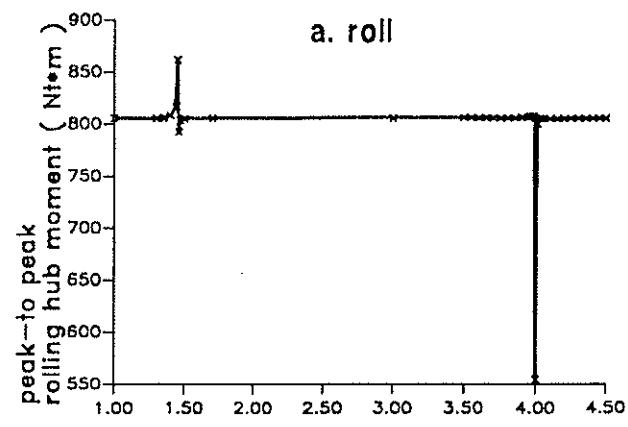
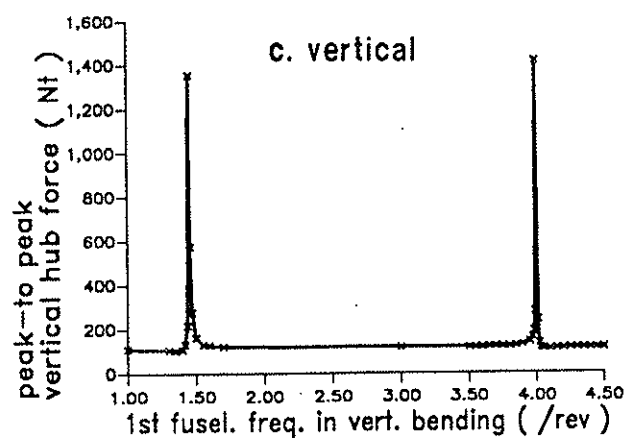
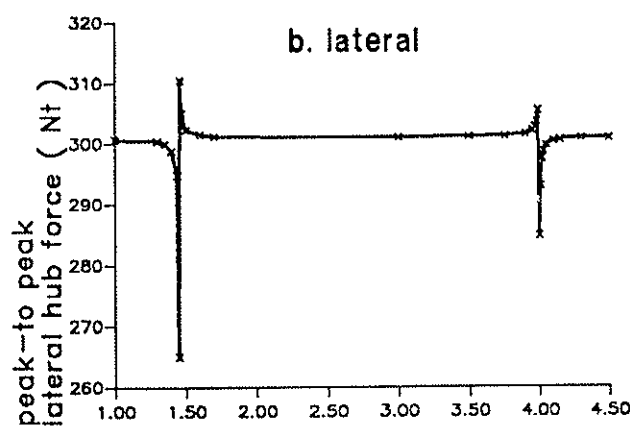
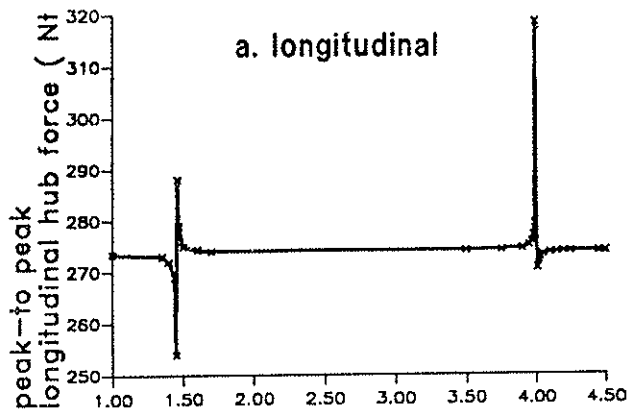


Figure 3: Variation of vibratory hub moments as a function of the fundamental fuselage natural frequency in vertical bending

Figure 2: Variation of vibratory hub shears as a function of the fundamental fuselage natural frequency in vertical bending

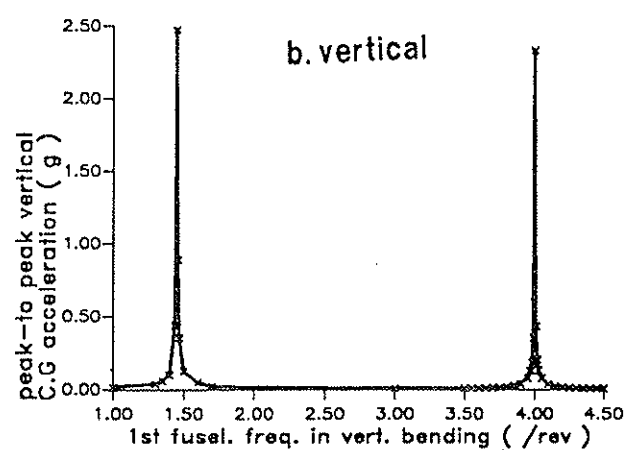
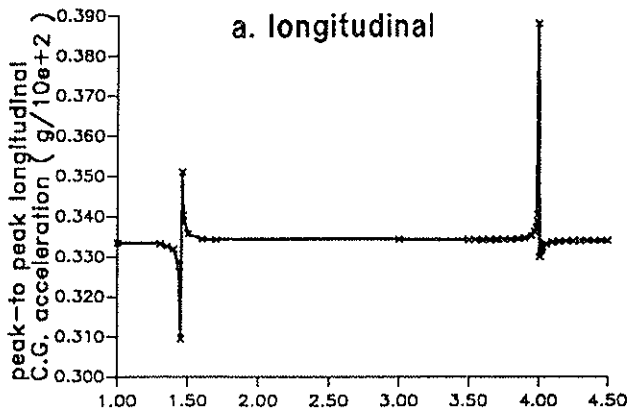
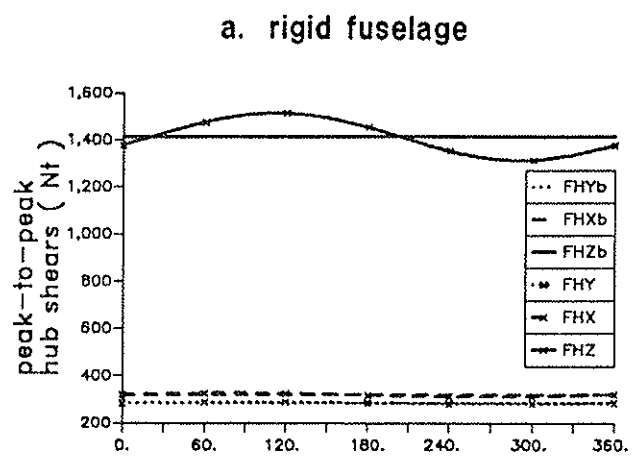
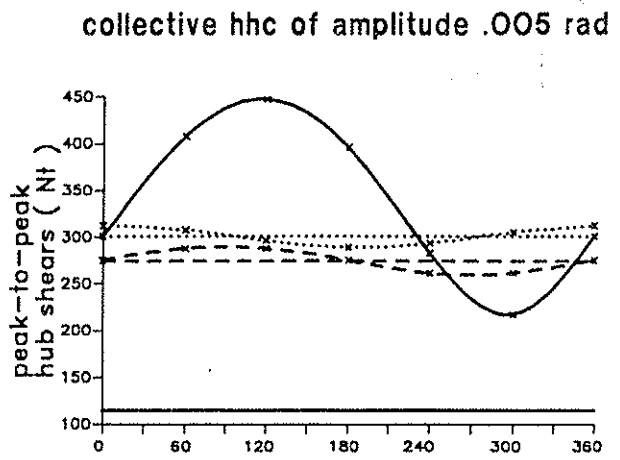
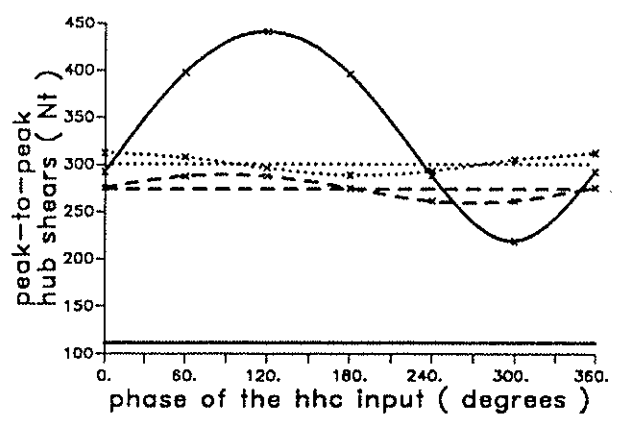


Figure 4: Variation of C.G. accelerations as a function of the fundamental fuselage natural frequency in vertical bending



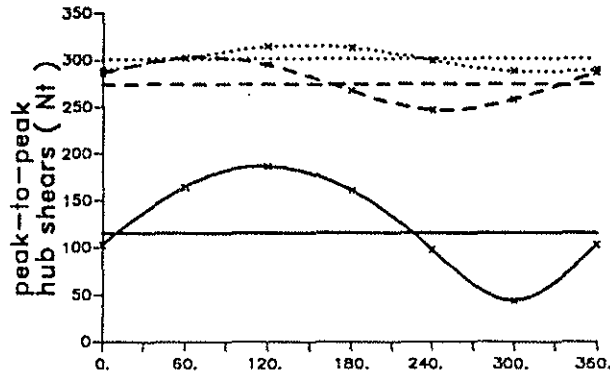
b. 1st vert. fus. bend. freq. = 4/rev



c. 1st vert. fus. bend. freq. = 1/rev

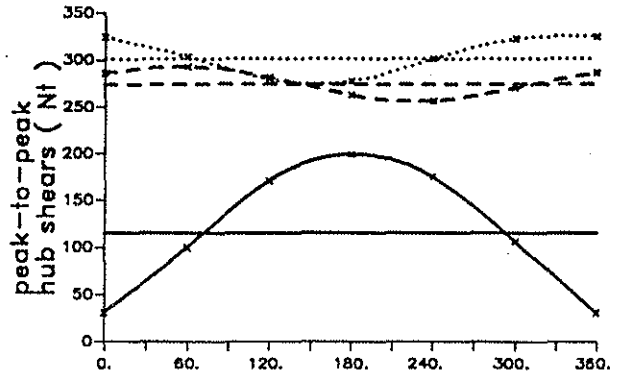
Figure 5: Influence of the collective HHC input on the vibratory hub shears

lateral hhc of amplitude .005 rad

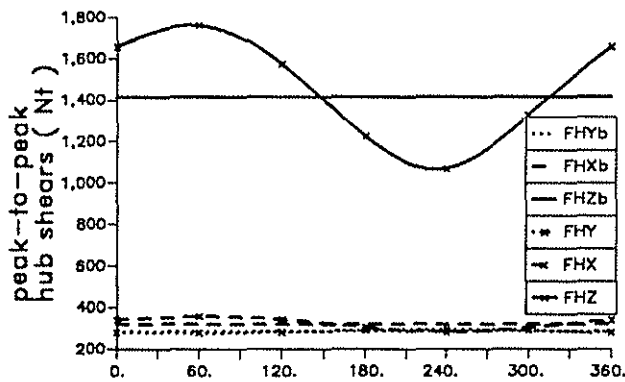


a. rigid fuselage

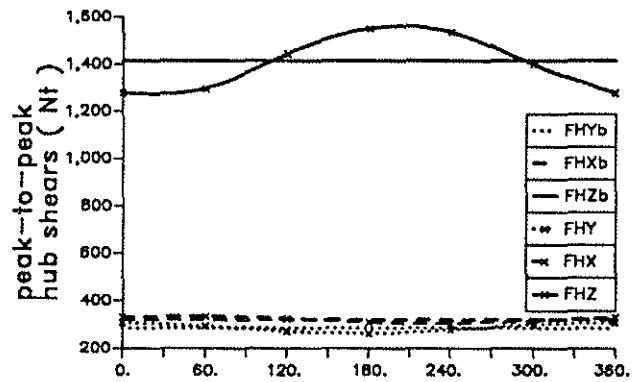
longitudinal hhc of amplitude .005 rad



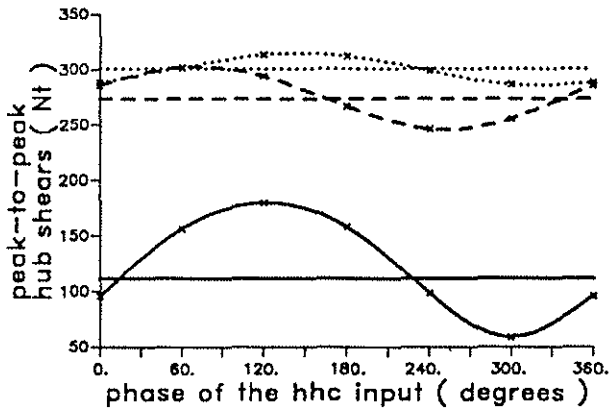
a. rigid fuselage



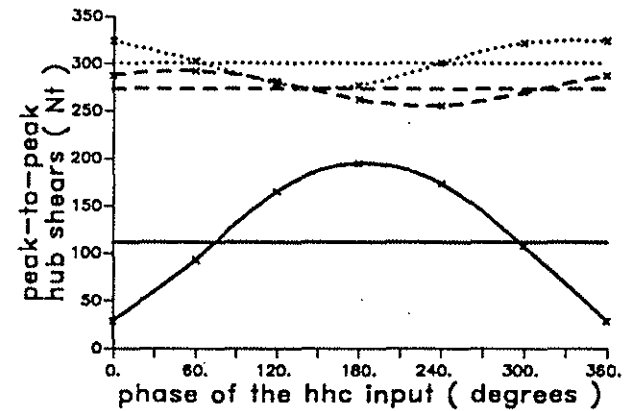
b. 1st vert. fus. bend. freq. = 4/rev



b. 1st vert. fus. bend. freq. = 4/rev



c. 1st vert. fus. bend. freq. = 1/rev

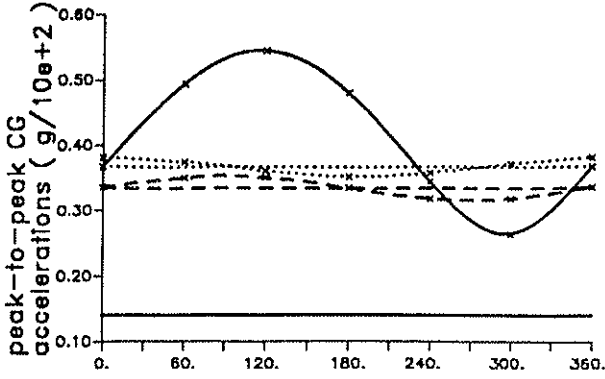


c. 1st vert. fus. bend. freq. = 1/rev

Figure 6: Influence of the lateral cyclic HHC input on the vibratory hub shears

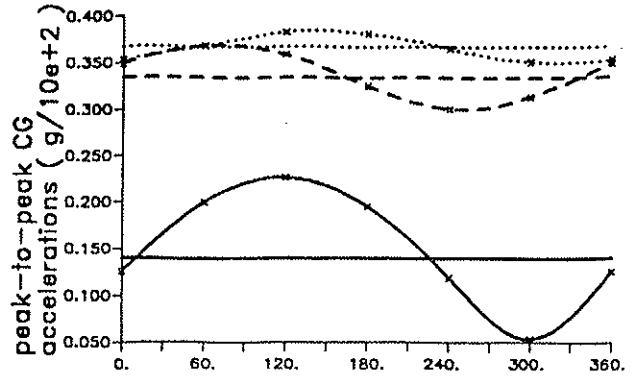
Figure 7: Influence of the longitudinal cyclic HHC input on the vibratory hub shears

collective hhc of amplitude .005 rad

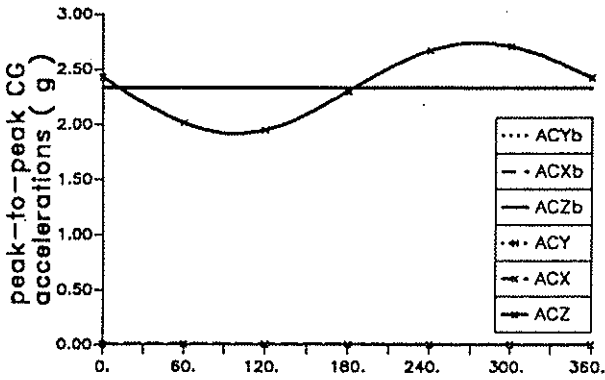


a. rigid fuselage

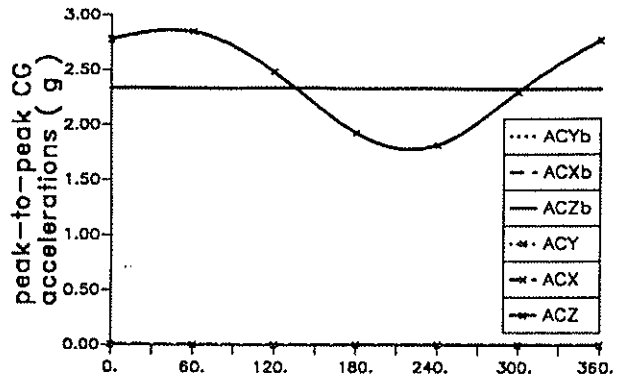
lateral hhc of amplitude .005 rad



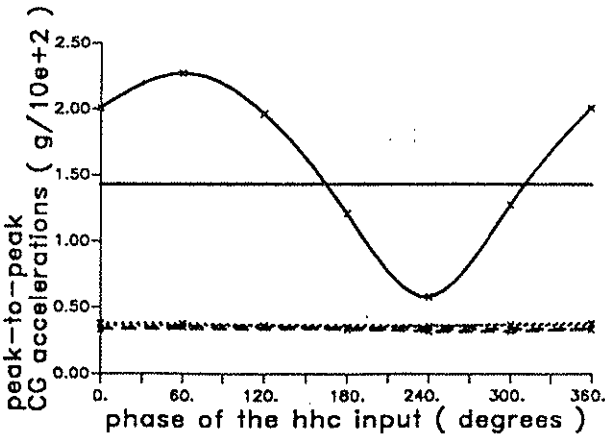
a. rigid fuselage



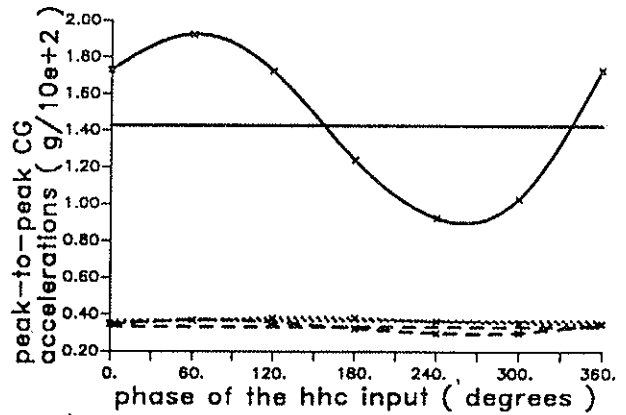
b. 1st vert. fus. bend. freq. = 4/rev



b. 1st vert. fus. bend. freq. = 4/rev



c. 1st vert. fus. bend. freq. = 1/rev

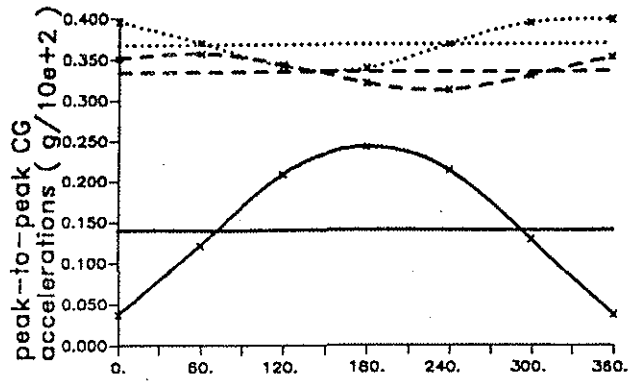


c. 1st vert. fus. bend. freq. = 1/rev

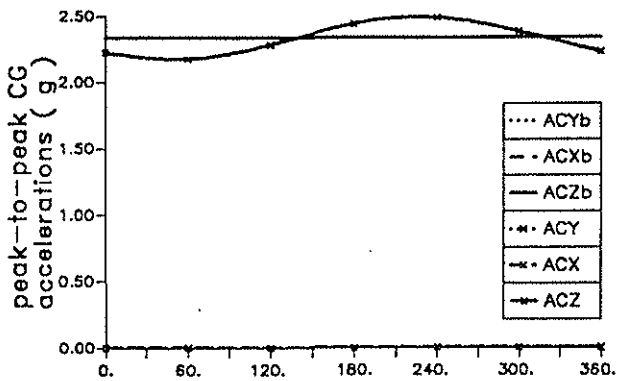
Figure 8: Influence of the collective HHC input on the C.G. accelerations

Figure 9: Influence of the lateral cyclic HHC input on the C.G. accelerations

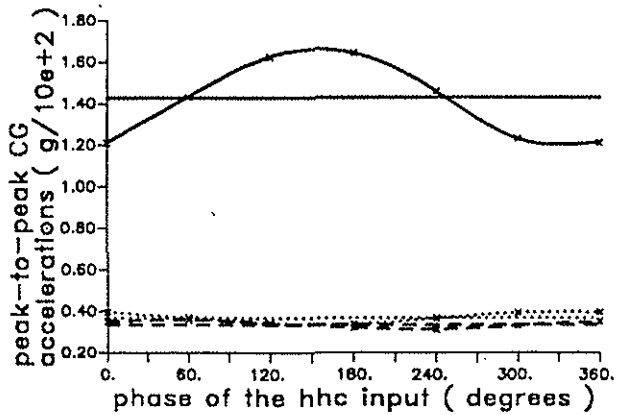
longitudinal hhc of amplitude .005 rad



a. rigid fuselage

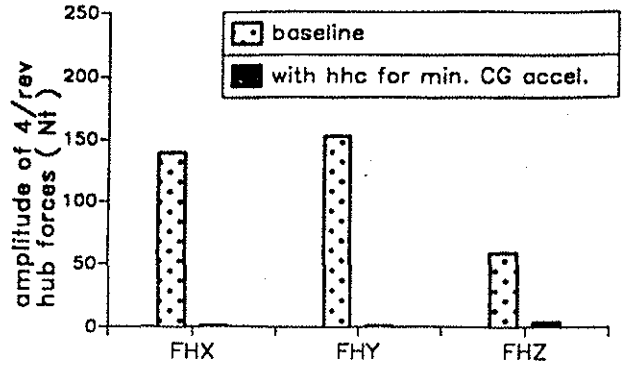


b. 1st vert. fus. bend. freq. = 4/rev

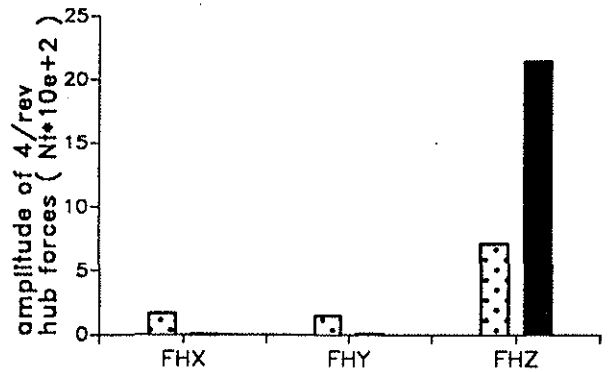


c. 1st vert. fus. bend. freq. = 1/rev

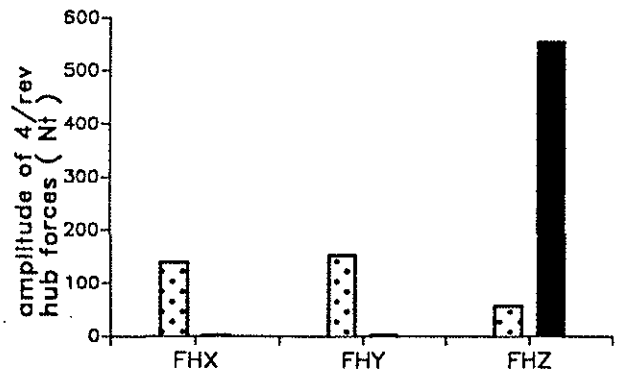
Figure 10: Influence of the longitudinal cyclic HHC input on the C.G. accelerations



a. rigid fuselage

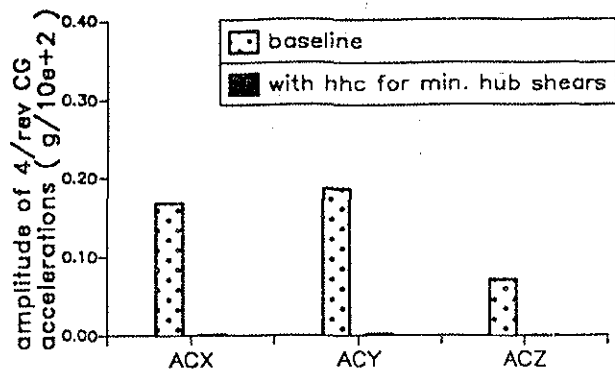


b. 1st vert. fus. bend. freq. = 4/rev

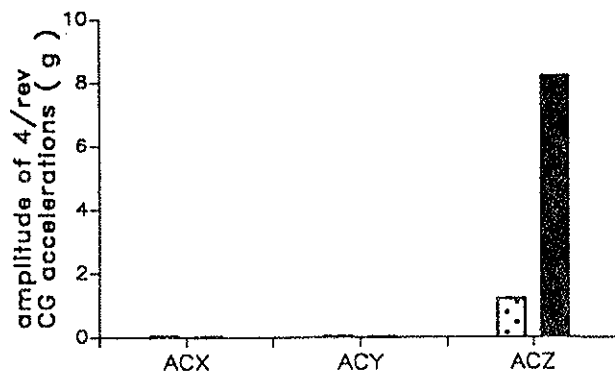


c. 1st vert. fus. bend. freq. = 1/rev

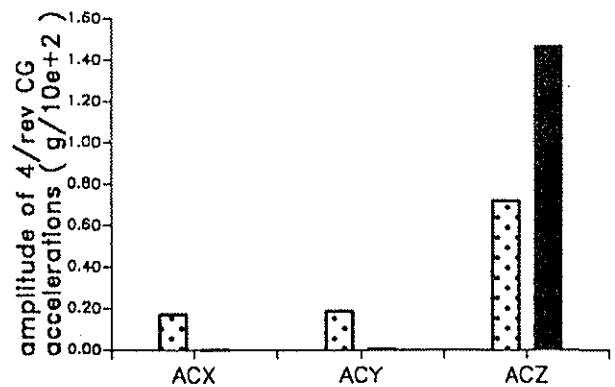
Figure 11: Effect of the HHC input for minimizing the C.G. accelerations on the hub shears



a. rigid fuselage



b. 1st vert. fus. bend. freq. = 4/rev



c. 1st vert. fus. bend. freq. = 1/rev

Figure 12: Effect of the HHC input for minimizing the hub shears on the C.G accelerations

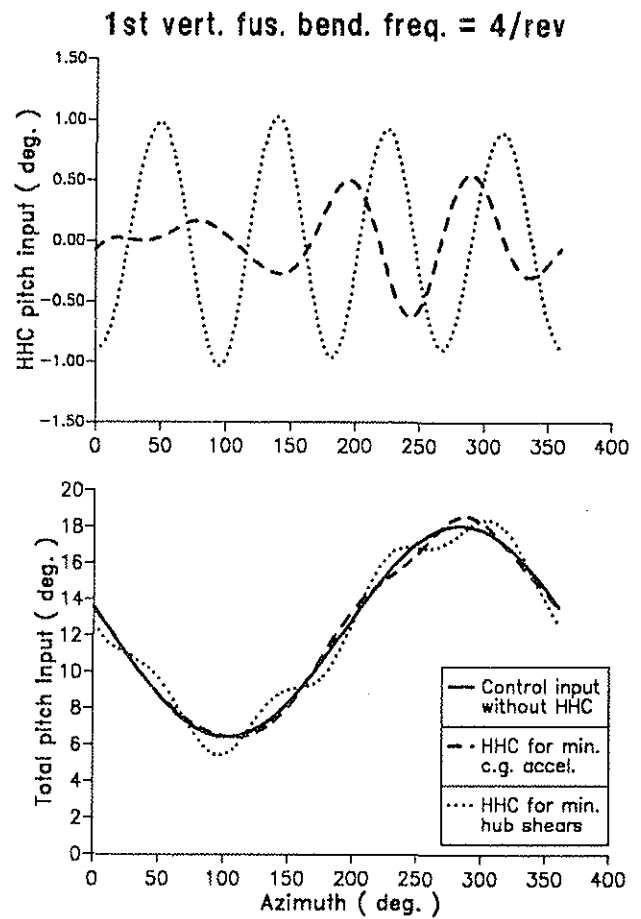


Figure 13: HHC inputs for minimizing the hub shears or the C.G. accel. in the rotating frame

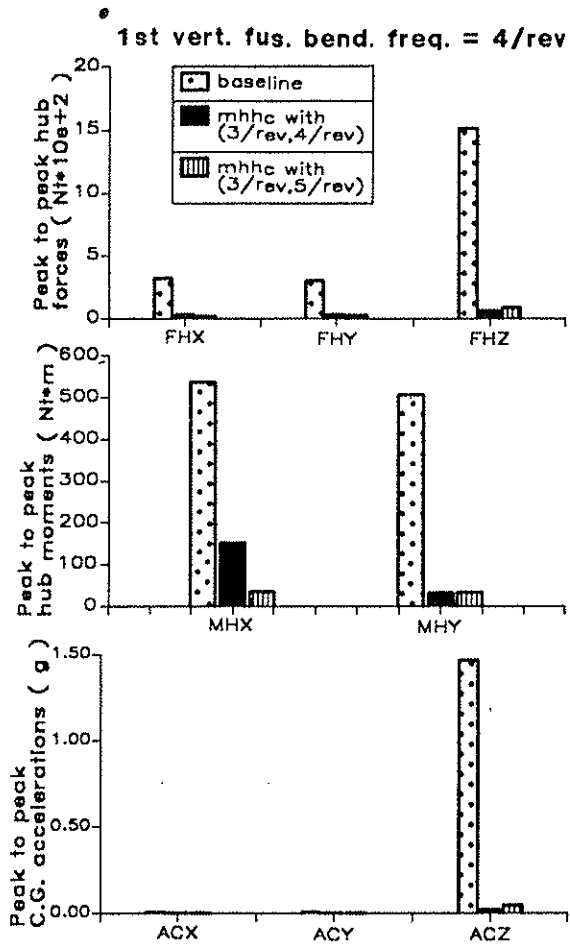


Figure 14: Hub shears, hub moments and C.G accelerations without HHC and with MHC (SBT)

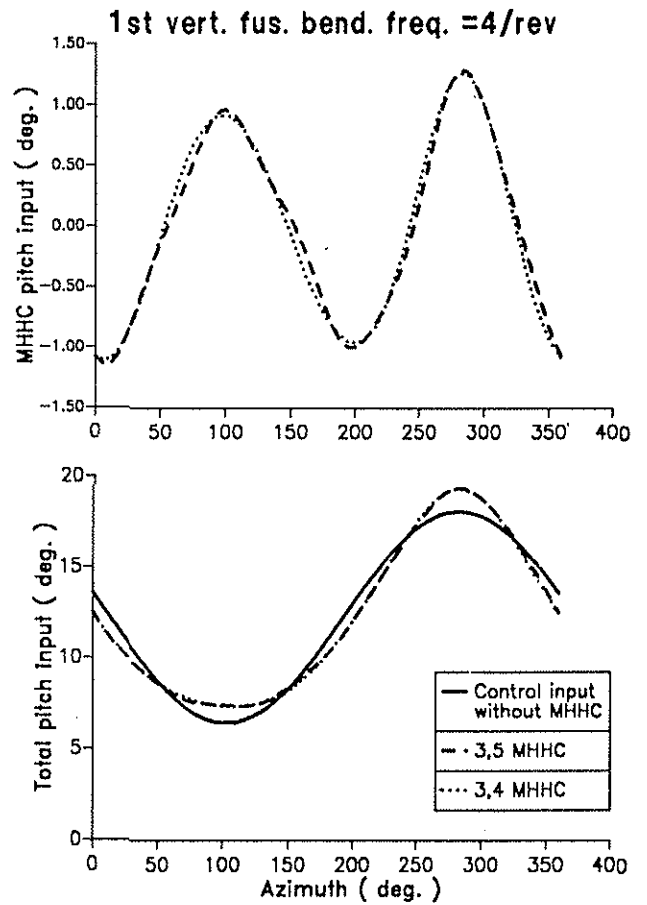


Figure 15: MHC pitch angle variation in the rotating frame for 3,4/rev and 3,5/rev combinations (SBT)

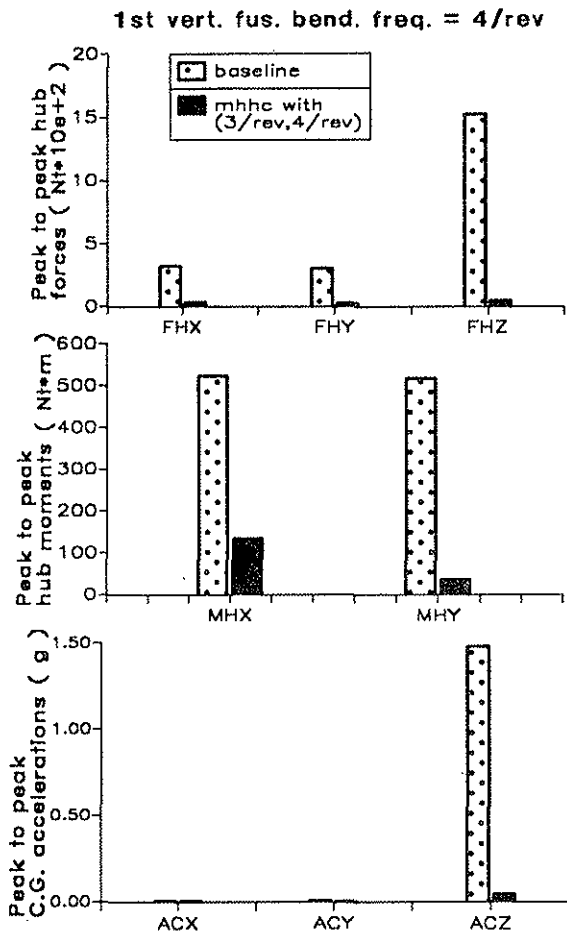


Figure 16: Hub shears, hub moments and C.G accelerations without HHC and with MHHc-(MBT)

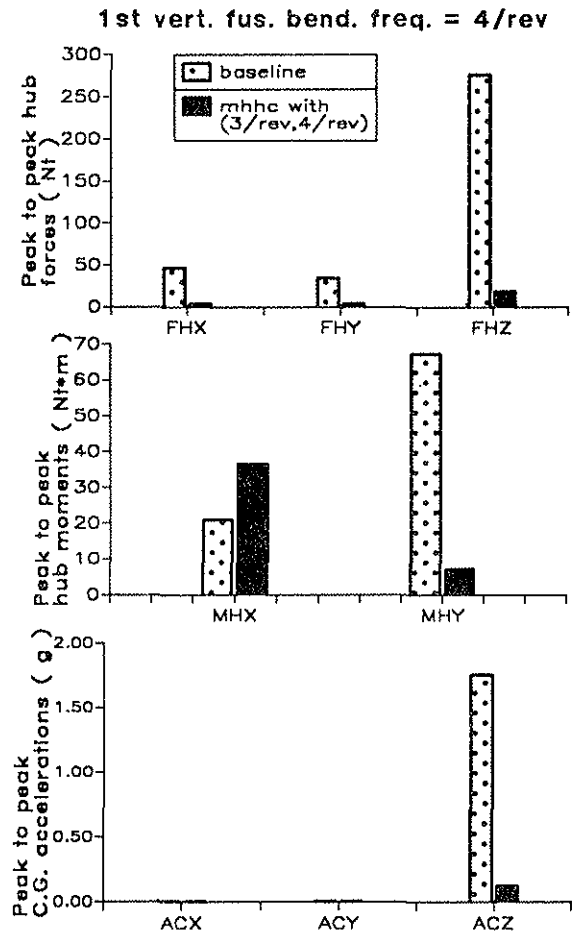


Figure 17: Hub shears, hub moments and C.G accelerations without HHC and with MHHc for MBB 105 (MBT)

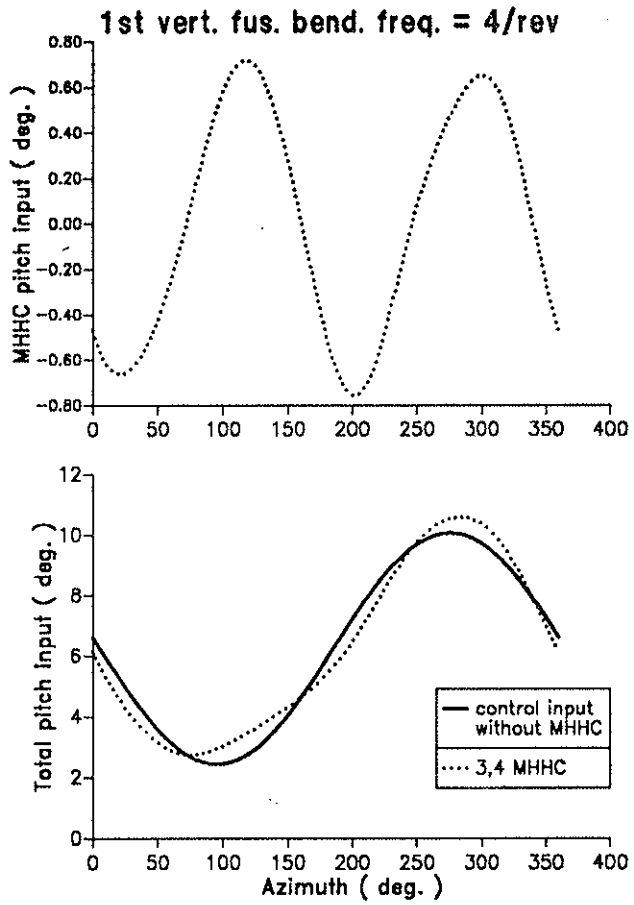


Figure 18: MHC pitch angle variation in the rotating frame with 3,4/rev combination for MBB 105 (MBT)